ISBN: 978-3-95450-247-9 ISSN: 2673-5490 doi: 10.18429/JACoW-IPAC2024-THPG42

RADIATION LEVELS IN THE LHC TUNNEL AND IMPACT ON ELECTRONICS DURING THE 2023 Pb ION RUN

A. Canesse*, D. P. Söderström, F. Cerutti, D. Di Francesca, S. Fiore, R. García Alía, G. Lerner, S. Niang†, E. Tagkoudi, D. Ricci, CERN, Geneva, Switzerland

Abstract

The 2023 operation of the Large Hadron Collider (LHC) at CERN included a one-month-long run with fully stripped Pb ion beams, marking the first heavy-ion run since 2018, and delivering Pb ion collisions at an unprecedented center-of-mass energy of 5.36 TeV per nucleon pair. During this period, the radiation fields in the LHC tunnel have been measured by means of different radiation monitors, including Beam Loss Monitors (BLMs), RadMons, and distributed optical fiber dosimeters, with the primary goal of quantifying the radiation exposure of electronic systems. The radiation levels are driven by the Bound Free Pair Production (BFPP) and Electromagnetic Dissociation (EMD) processes taking place in all four interaction points, yielding significant radiation peaks in the Dispersion Suppressor (DS) regions of the tunnel. An overview of the radiation levels is presented in this contribution, with a special focus on the Insertion Region 2 (IR2) hosting the ALICE experiment, where the new Target Collimator Long Dispersion suppressor (TCLD) has been installed specifically for the ion run. The impact of radiation on the electronic systems and on the LHC availability during the run will also be discussed.

INTRODUCTION

During the operation of the Large Hadron Collider (LHC) [1] at CERN, beam losses produce a mixed radiation field that can damage electronic systems in the form of cumulative lifetime degradation, or stochastic Single-Event Effects (SEEs) [2]. These effects can cause unwanted LHC beam dumps and downtime, and must be mitigated via equipment relocations, shielding, or radiation hard designs. The radiation levels at CERN accelerators are actively monitored in the context of Radiation to Electronics (R2E) activities. Previous studies reported the LHC radiation levels in 2022 [3], during Run 2 [4], and in the injector chain [5]. This article presents an overview of the levels during the 2023 LHC ion run, where the beam loss pattern differs from proton operation due to different beam properties and parameters.

LHC Layout

The LHC is divided into eight Insertion Regions (IR) and eight arc sections, each connected by the Dispersion Suppressor (DS) regions [1]. The beamline is further subdivided into half-cells: the IR straight sections go from half-cells 1 to 7, the DS from 8 to 12, and arcs from 13 to 34. Four of the IRs host Interaction Points (IPs) where the two LHC beams collide at the center of four different detectors: ATLAS (IP1), ALICE (IP2), CMS (IP5), and LHCb (IP8). Other IRs host components to operate the accelerator such as momentum (IR3) and betatron (IR7) collimators. The main sources of radiation in the LHC tunnel depend on the location. In the IRs, radiation mostly originates from inelastic collisions at the IPs, and it scales with delivered luminosity (Table 1). In the arcs, radiation is mostly driven by beam-gas interactions and scales with beam intensity and residual gas density [3].

Table 1: Integrated and Peak Instantaneous Luminosities Delivered to LHC Experiments During Pb-Pb Ion Runs [6]

	Integrated [nb^{-1}]			**Peak [10^{27}cm^{-2}s^{-1}]**		
	2015	2018	2023	2015	2018	2023
IP1	0.58	1.80	1.91	2.89	6.13	5.82
IP2	0.43	0.91	2.16	1.47	1.30	6.42
IP5	0.59	1.80	2.02	3.17	6.09	5.87
IP8	6.2e-3	0.24	0.25	0.10	1.59	0.87

Ion Beams

In 2015, 2018, and 2023, the LHC collided beams of fully stripped lead ions ($^{208}Pb^{82+}$). Operational challenges during Pb-Pb operation come from luminosity-driven processes taking place at the IPs [7]:

- Bound-free pair production (BFPP), where secondary $^{208}Pb^{81+}$ beams are emitted from the IPs, leading to localized losses in the DS region:

$$^{208}\,Pb^{82+} + {}^{208}\,Pb^{82+} \rightarrow {}^{208}\,Pb^{82+} + {}^{208}\,Pb^{81+} + e^{+} \quad (1)$$

- Electromagnetic dissociation (EMD), where a nucleus loses nuclear fragments. Most interactions involve the emission of 1 or 2 neutrons, leading to the loss of secondary beams ($^{207}Pb^{82+}$ or $^{206}Pb^{82+}$) in the DS region.

In IR1 and IR5, the LHC beam optics would cause the BFPP beam to be lost at the second superconducting dipole of half-cell 11 in the DS, and an orbit bump is used to shift the impact point further downstream to an empty cryostat. Instead, in IR2, the optics would only allow losing the BFPP beam in half-cell 10 or 12, so it was decided to install additional TCLD collimators in half-cell 11 during LS2 to protect the half-cell 12 magnets [8]. In IR8, collision-driven losses are less critical because the LHCb experiment typically receives less ion luminosity than ATLAS, ALICE, and CMS.

* auriane.canesse@cern.ch
† Presenter

ISBN: 978-3-95450-247-9 ISSN: 2673-5490 doi: 10.18429/JACoW-IPAC2024-THPG42

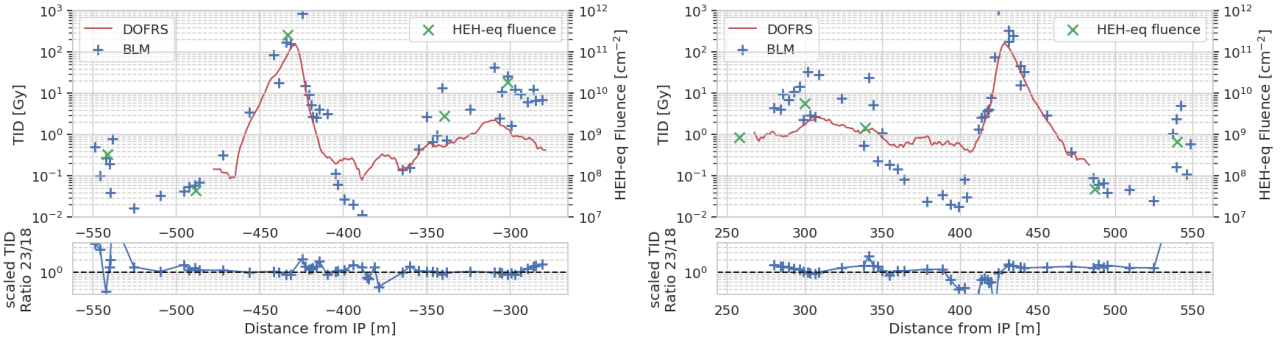

Figure 1: Radiation levels in point 1 DS after the 2023 ion run. TID (left axis) was measured both by BLMs and DOFRS. HEH-eq fluence (Right Axis) was measured by RadMons. The bottom plot shows the comparison with the 2018 ion run.

DATA ACQUISITION

Three detector types are used for radiation level monitoring and the data is pre-processed by an automated radiation level analysis system [9].

Beam Loss Monitors (BLMs) are ionization chamber detectors initially developed for machine protection [10]. Periodically located outside of the LHC magnet cryostats, they measure the Total Ionizing Dose (TID) in N_2 and cover a high dynamic range of over 10^9.

The RadMon system is designed to measure TID, High Energy Hadrons equivalent (HEH-eq) and thermal neutron fluences to assess their impact on electronic systems [11]. In the LHC tunnel, RadMons are typically located on the floor below the LHC magnets. They can host a deported module to measure TID at a further location.

The Distributed Optical Fiber Radiation Sensing (DOFRS) system [12] uses several silica-based radiation-sensitive optical fibers to measure TID. The fibers are deployed in the DS regions of IR1, IR5, and IR7 along the accelerator tunnel walls at approximately constant distance from the beam-pipe. The Radiation Induced Attenuation (RIA) of each fiber is read out by optical time domain reflectometers (OTDR). The DOFRS used in this study have a minimal resolution and detection limit of ~1 Gy.

2023 PB ION RUN RADIATION LEVELS

Arcs Regions

In the LHC arcs, the TID is measured by BLMs located periodically on the main LHC magnets. The average TID during the 2023 ion run varied from 3 mGy to 14 mGy, as shown in Table 2. Higher TID levels were reached in the 2023 proton run due to the higher beam intensity. TID spikes caused by localized beam losses in the arcs were observed during the ion run and reached a maximum of ~1 Gy, while losses during the proton run could reach ~10 Gy.

Dispersion Suppression (DS) Regions

The DS regions of the IRs hosting IPs are the most critical for R2E during ion runs due to BFPP and EMD losses. Indeed, the radiation levels measured during the 2023 ion run reflect the expected loss pattern for these processes.

Table 2: Average and Maximum BLM TID Measurement in the LHC Arcs in 2023

	Ion Run [mGy]		Proton Run [mGy]	
Arc	**mean**	**max**	**mean**	**max**
12	12	1158	68	4730
23	3.8	60	82	10527
34	3.1	98	31	135
45	5.6	102	65	3554
56	6.6	408	68	3550
67	14	588	30	185
78	4.2	33	61	4128
81	5.8	329	57	1539

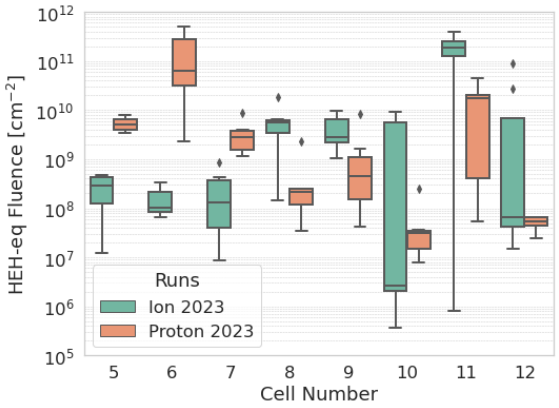

Figure 2: HEH-eq fluence in cells 5-12 around IPs 1, 2, 5, 8 measured during 2023 ion (green) and proton (red) runs.

Figure 1 shows TID and HEH-eq fluence profiles in the DS of IR1. The BFPP loss peak at 430 m (in half-cell 11) on both sides of the IP is observed by all radiation monitors. Within the 350-400 m range, the BLMs measure low radiation levels that fall below the DOFRS system detection limit of 1 Gy (hence the latter measurements are interpreted as overestimated). Figure 2 shows the HEH-eq fluence for the DS and half-cells 5-7 of the straight sections of IRs 1, 2, 5, and 8. In half-cells 5-7, the average HEH-eq fluence was significantly higher during the proton run because of its

ISBN: 978-3-95450-247-9 ISSN: 2673-5490 doi: 10.18429/JACoW-IPAC2024-THPG42

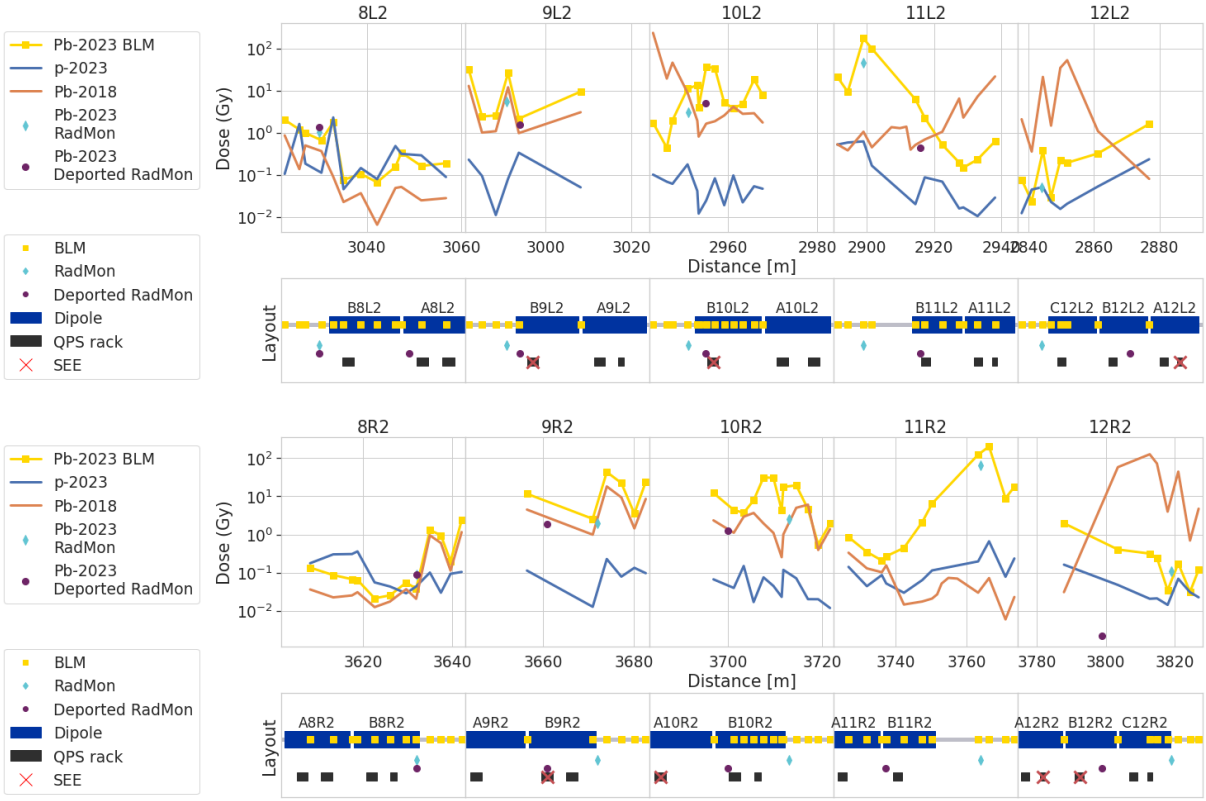

Figure 3: Cumulative TID in the DS on the left (top) and right (bottom) of IP2 for the 2018 and 2023 ion runs, and for the 2023 proton run. The location of LHC dipoles, radiation monitors, QPS racks, and 2023 QPS faults is also shown.

much higher integrated luminosity. In the DS, the opposite trend is observed in half-cells 11 and 12 due to BFPP and EMD losses in the ion run.

Figure 3 shows the measured TID in the DS of IR2 (ALICE) for the Pb ion runs of 2018 and 2023, and for the 2023 proton run. The measurements are mostly obtained with BLMs, but the 2023 RadMons (and deported modules) located at floor level show consistent results when available. As expected, a much larger cumulative TID is observed in the DS during both 2018 and 2023 Pb ion runs compared to the 2023 proton run, due to the BFPP and EMD processes. However, the position of the TID peaks has moved from half-cell 12 (on the right of IP2) and 10 (on the left) in 2018 to half-cell 11 in 2023, due to the installation of the new TCLD collimators [8].

QPS Faults During the 2023 Ion Run

The Quench Protection System (QPS) protects the LHC magnets by triggering beam dumps before any magnet quenches can occur [13]. The system includes electronic racks distributed periodically below the LHC dipoles in the DS and arc regions, and due to its criticality, any severe malfunctioning is set to automatically prevent the LHC operation. During the 2023 ion run, 13 QPS faults attributed to SEEs in QPS racks led to premature LHC beam dumps and, as a result, to a loss of LHC availability. The location of SEE events is detailed in Table 3, showing that most of them (9) occurred in the IR2 DS. While a full analysis of these faults is beyond the scope of this paper, their increase can be explained by the different TID distribution in the IR2 DS in the 2023 ion run compared to past operation (Figure 3) and the higher ALICE integrated luminosity in 2023 (Table 1).

Table 3: QPS R2E Faults Locations During 2023 Ion Run

Half-cells	8L5	9L2	9R2	10L2	10R2
#SEE	1	1	1	3	1
Half-cells	11L1	12R1	12L2	12R2	
#SEE	1	2	1	2	

CONCLUSION

Radiation levels were measured at the LHC during the 2023 ion run.While the arc levels are much lower than during proton operation, BFPP and EMD interactions specific to ion collisions lead to increased losses in the DS of the IRs hosting IPs. The installation of new TCLD collimators in IR2 shifted the main loss peaks from half-cells 10-12 (in the 2018 ion run) to half-cell 11 (in 2023). A total of 13 beam dumps were triggered by SEEs in QPS racks during the 2023 ion run, which can be at least partially attributed to the increased ALICE luminosity (leading to higher overall losses) and the different TID distribution in the IR2 DS.

ISBN: 978-3-95450-247-9 ISSN: 2673-5490 doi: 10.18429/JACoW-IPAC2024-THPG42

REFERENCES

[1] O. Brüning *et al.*, "LHC Design Report.", CERN, 2004. doi:10.5170/CERN-2004-003-V-1

[2] S. De Carvalho *et al.*, "Radiation Environments and their Impact at the CERN's Injector Chain"CERN, Geneva, Switzerland, Rep. CERN-ACC-NOTE-2015-0042, Dec. 2015. https://cds.cern.ch/record/2114889

[3] K. Bilko, R. Garcia Alia, S. Girard, and M. Sebban, "Overview of total ionizing dose levels in the Large Hadron Collider during 2022 restart", in *Proc. IPAC'23*, Venice, Italy, May 2023, paper THPA047, pp. 4059–4062. doi:10.1109/TNS.2023.3328145

[4] Y. Q. Aguiar *et al.*, "Radiation to Electronics Impact on CERN LHC Operation: Run 2 Overview and HL-LHC Outlook", in *Proc. IPAC'21*, Campinas, Brazil, May 2021, pp. 80–83. doi:10.18429/JACoW-IPAC2021-MOPAB013

[5] A. Canesse *et al.*, "Overview of the radiation levels in the CERN accelerator complex after LS2", in *Proc. IPAC'23*, Venice, Italy, May 2023, pp. 4055–4058. doi:10.18429/JACoW-IPAC2023-THPA046

[6] LHC Programme Coordination, https://lpc.web.cern.ch/.

[7] M. Schaumann *et al.*, "Bound-free pair production from nuclear collisions and the steady-state quench limit of the main dipole magnets of the CERN Large Hadron Collider", *Phys. Rev. Accel. Beams*, vol. 23, no. 12, Dec. 2020. doi:10.1103/PhysRevAccelBeams.23.121003

[8] ALICE collaboration, "Upgrade of the ALICE Experiment: Letter Of Intent", *J. Phys. G*, vol. 41, no. 8, p. 087001, 2014. doi:10.1088/0954-3899/41/8/087001

[9] K. Biłko, R. García Alía, and J. B. Potoine, "Automated Analysis of the Prompt Radiation Levels in the CERN Accelerator Complex", in *Proc. IPAC'22*, Bangkok, Thailand, Jun. 2022, pp. 736–739. doi:10.18429/JACoW-IPAC2022-MOPOMS043

[10] B. Dehning *et al.*, "The LHC Beam Loss Measurement System", in *Proc. PAC'07*, Albuquerque, NM, USA, Jun. 2007, paper FRPMN071, pp. 4192–4194.

[11] G. Spiezia *et al.*, "A new RadMon version for the LHC and its injection lines", *IEEE Trans. Nucl. Sci.*, vol. 61, no. 6, pp. 3424–3431, Dec. 2014. doi:10.1109/TNS.2014.2365046

[12] D. Di Francesca *et al.*, "Dosimetry Mapping of Mixed-Field Radiation Environment Through Combined Distributed Optical Fiber Sensing and FLUKA Simulation", *IEEE Trans. Nucl. Sci.*, vol. 66, no. 1, pp. 299–305, Jan. 2019. doi:10.1109/TNS.2018.2882135

[13] T. Podzorny *et al.*, "Quench Protection System", in *9th LHC Operations Evian Workshop*, pp. 143–148, Feb. 2019. https://cds.cern.ch/record/2750290